arXiv:1212.0731v1 [cond-mat.soft] 4 Dec 2012

Multivalent ion effects on electrostatic stability of virus-like nano-shells

Leili Javidpour,[1] Anže Lošdorfer Božič,[2] Ali Naji,[1, 3, *] and Rudolf Podgornik[2, 4, 5]

[1]*School of Physics, Institute for Research in Fundamental Sciences (IPM), Tehran 19395-5531, Iran*
[2]*Department of Theoretical Physics, Jožef Stefan Institute, SI-1000 Ljubljana, Slovenia*
[3]*Department of Applied Mathematics and Theoretical Physics, University of Cambridge, Centre for Mathematical Sciences, Cambridge CB3 0WA, United Kingdom*
[4]*Department of Physics, Faculty of Mathematics and Physics, University of Ljubljana, SI-1000 Ljubljana, Slovenia*
[5]*Department of Physics, University of Massachusetts, Amherst, MA 01003, USA*

Electrostatic properties and stability of virus-like nano-shells are examined in mixed ionic solutions with monovalent and multivalent ions. A theoretical model based on a thin charged sphere and multivalent ions within the "dressed multivalent ion" approximation is compared with extensive implicit Monte-Carlo simulations and shown to be accurate for positive or low negative surface charge density of the shell, and for sufficiently high (low) monovalent (multivalent) salt concentrations. Deviations between simulation and theory occur due to many-body effects leading to formation of a strongly correlated layer of vicinal ions. Phase diagrams of electrostatic (osmotic) pressure show positive and negative pressure values, corresponding to outward and inward facing forces on the shell, providing an explanation for high sensitivity of viral shell stability on the ionic environment.

Electrostatic interactions contribute a significant part to the total free energy of charged viral capsids and/or virus-like shells [1]. In this context multivalent ions behave rather differently from monovalent ones. Some of the major functions of multivalent metal ions such as Mg^{2+}, Zn^{2+}, and Ca^{2+} are surmised to enhance the capsid stability, enable their conformational alterations [2] or assist in the genome packaging [3], while multivalent polyamines like spermine (Spm^{4+}) are required for a proper stabilization of viruses [4, 5]. Though Rossman and Eriksson, already a while ago, clearly associated swelling of capsids with the removal of multivalent ions [6], the exact mechanism of electrostatic capsid destabilization remains to a large extent elusive. Here we suggest a rather universal mechanism that could underline the action of multivalent ions on viral capsid stability.

In order to properly understand the nature of electrostatic interactions in viruses, we investigate the effects of highly charged bathing solution ions on the capsid stability *via* their spatial distribution and the associated (osmotic) pressure. To accomplish this goal and analyze the distribution of highly charged ions in the vicinity of charged capsid shells, the Poisson-Boltzmann (PB) *paradigm*, valid only for weakly charged or highly screened Coulomb systems, has to be properly amended [7]. This is achieved in a twofold manner: by formulating an analytical "dressed multivalent-ion approach" [8], as well as by combining it with exhaustive Monte-Carlo (MC) simulations within a simple model in order to properly capture the salient characteristics of electrostatic effects on capsid stability.

Consider a closed spherical shell of radius R and surface charge density σ, Fig. 1a, which may serve as a reasonable model for a wide range of viral capsids such as brome mosaic virus, cowpea chlorotic mottle virus, etc., [9, 10] as well as synthetic nano-shells [11, 12], whose effective radius and surface charge density can both be extracted from experimental data. For typical viruses, these values fall in the range 2.5 nm $\lesssim R \lesssim$ 30 nm with thicknesses between 2 and 4 nm and $|\sigma| \lesssim 0.4\ e_0/\mathrm{nm}^2$. There is no clear-cut preference for inner-outer capsid surface charge density sign segregation and in fact both signs are admissible [10]. The shell is considered to be permeable to ions and immersed in an ionic solution comprising a monovalent $1:1$ salt of bulk concentration n_0 and a multivalent $q:1$ salt of bulk concentration c_0, where q is the charge valency of multivalent ions.

The above model presents an asymmetric multicomponent Coulomb system which is not amenable to exact analytical treatment. We therefore resort to the "dressed multivalent-ion approximation" [8], which can be derived as an approximate theory from a systematic field-theoretical formalism in situations where the ionic mixture is highly asymmetric, i.e., $q > 1$. In this approach, the degrees of freedom associated with monovalent ions are integrated out from the partition function, resulting in an effective formalism incorporating only screened Debye-Hückel (DH) interactions between the remaining "dressed" multivalent ions and fixed (macroion) surface charges [8]. On this level, the problem is still a many-body one but it can be treated with fast and efficient MC simulations as one needs to include only the dressed ions' degrees of freedom. In order to proceed with an analytical theory, however, it turns out that the grand-canonical partition function of the system can be expanded in terms of the fugacity (concentration) of multivalent ions, which is indeed small in most cases of experimental interest [4, 13]. To the leading order, this procedure then leads to the *dressed multivalent-ion theory* containing the lowest order contribution from the interaction between dressed multivalent ions and fixed macroion charges in the system. The dressed multivalent-ion theory is thus

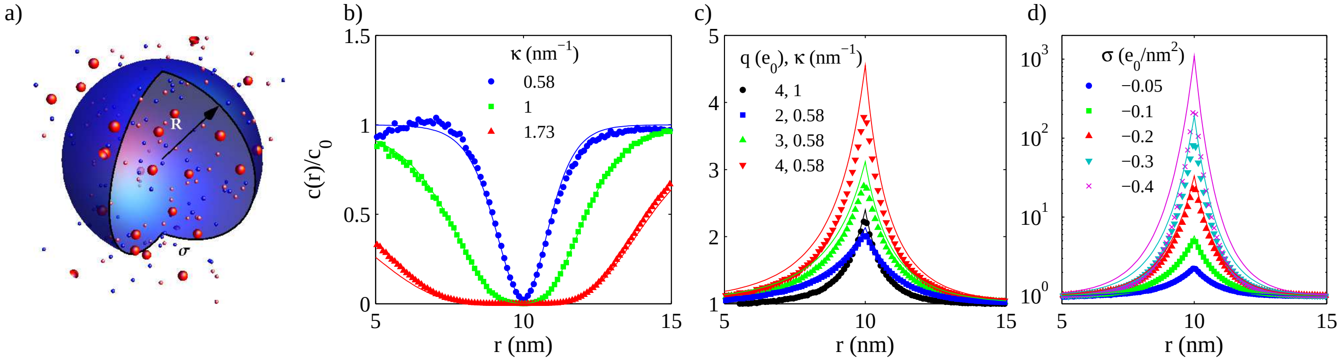

FIG. 1: (Color online) a) Schematic view of a spherical shell of radius R and surface charge density σ immersed in a mixed solution comprising mono- and multivalent salt ions (multivalent ions are shown by bigger red spheres). b) Rescaled density of multivalent ions, $c(r)/c_0$, in the vicinity of a charged shell with radius $R = 10$ nm as a function of the radial distance r from the center of the shell. Symbols show MC simulation data and lines the analytical dressed multivalent-ion predictions for $\sigma = +0.4$ e_0/nm^2, $q = 4$, and various κ as indicated on the graph. c) Same as (b) but for $\sigma = -0.05$ e_0/nm^2, and κ and q values as shown on the graph, and d) for $\kappa = 1$ nm^{-1}, $q = 4$, and different values of (negative) σ. In all cases, we have $qn_0 = 4$ mM.

related to the *strong-coupling theory*, introduced originally for salt-free systems containing only multivalent counterions [7]. It has been tested extensively against all-ion (explicit) MC simulations and has been shown to be a valid theory for moderately large values of q and monovalent salt concentration n_0, and for sufficiently low concentration of multivalent salt c_0 [8, 14].

For a charged shell, one can express the dressed multivalent-ion free energy of the system as follows [8, 14]

$$\beta\mathcal{F} = \beta\mathcal{F}_{DH} - c_0 \int \mathrm{d}\mathbf{r}\, e^{-\beta q e_0 \varphi_{DH}(\mathbf{r})} + \mathcal{O}(c_0^2), \tag{1}$$

where $\beta = 1/(k_{\mathrm{B}}T)$ and the first term is the self-energy of the charged shell in the DH limit, i.e., in the absence of multivalent ions, which can be calculated as in Ref. 15. The integral in the second term corresponds to the partition function for the single-particle DH interaction of a multivalent ion with the charged shell, with $\varphi_{DH}(\mathbf{r})$ being the screened electrostatic potential of the shell, which follows simply from the DH equation $\nabla^2\varphi_{DH}(\mathbf{r}) = \kappa^2\varphi_{DH}(\mathbf{r})$ solved in the presence of the charged permeable shell. Note that the inverse Debye screening length κ depends on the bulk concentrations of both mono- and multivalent ions as $\kappa^2 = 8\pi\ell_{\mathrm{B}}(n_0 + qc_0/2)$, where $\ell_{\mathrm{B}} = \beta e_0^2/(4\pi\varepsilon\varepsilon_0)$ is the Bjerrum length.

The (number) density of multivalent ions is then

$$c(\mathbf{r}) = c_0 \,\exp\big(-\beta q e_0 \varphi_{DH}(\mathbf{r})\big), \tag{2}$$

and the electrostatic (osmotic) pressure acting on the shell is obtained as $P = -\partial\mathcal{F}/\partial V$, or

$$P = P_{DH} + P_q = -\frac{\partial\mathcal{F}_{DH}}{\partial V} + k_{\mathrm{B}}Tc_0\,\frac{\partial}{\partial V}\int \mathrm{d}\mathbf{r}\, e^{-\beta q e_0\varphi_{DH}(\mathbf{r})}, \tag{3}$$

where $V = 4\pi R^3/3$ is the shell volume, and the partial derivatives are taken at *fixed total charge* $Q_\sigma = 4\pi\sigma R^2$. The pressure can thus be divided into two parts, one stemming from the self-energy of the charged shell P_{DH}, and the other one from the multivalent ions. The former contribution is purely *positive* but the latter can become *negative* as we explain later. The explicit forms of $\varphi_{DH}(\mathbf{r}) = \varphi_{DH}(r)$ and $\mathcal{F}_{DH}$ can be found in Ref. 15.

In order to assess the validity of the dressed multivalent-ion theory detailed above we have used extensive MC simulations in which we simulate a large collection of mobile (dressed) multivalent ions near a charged permeable shell with the monovalent ions being treated implicitly. This means that multivalent ions as well as the fixed charges on the shell interact through the screened DH interaction pair potential. The monovalent salt concentration, n_0, is varied in the range between 30 mM to 300 mM and we typically take a small multivalent salt concentration c_0 of a few mM in accordance with virus experiments [4, 13]. We use canonical MC simulations for dressed multivalent ions (assumed to be confined in a sufficiently large outer cubic volume with the charged shell located at the center), but employ an iterative method to produce a constant equilibrium "bulk" concentration of multivalent ions of a given value at large separations from the capsid [16], which thus effectively simulates an open (grand-canonical) system. In what follows, we shall take *positively* charged multivalent ions with $q = 2$, 3, 4, the ambient temperature $T = 300$ K, and the dielectric constant as that of water, $\varepsilon = 80$.

In Fig. 1, we show the rescaled number density profile of multivalent ions in the vicinity of a charged shell of radius $R = 10$ nm as a function of the radial distance from the center of the shell. In certain regimes of parameters the analytical prediction from the dressed multivalent-ion theory [Eq. (2), shown by solid lines] performs very well and closely matches the MC simulation results (symbols). For positively charged shells, $\sigma > 0$, there is always an excellent agreement showing a drop in the density of ions close to the shell surface (Fig. 1b). For negative σ, however, multivalent ions are attracted and accumulate more strongly at the shell surface. There is still a wide range of parameters where theory and MC simulations quantitatively agree (Figs. 1c and d, e.g., for divalent ions and the DH screening length $\kappa = 0.58$ nm^{-1} corresponding to a 30 mM monovalent salt concentration). In fact, as shown in Fig. 1b, by increasing q, the multivalent ion density at the surface increases but at the same time deviations between the simulations and the analytical predictions tend to grow. This implies an incipient role for multi-particle correlations which are absent in the theory. In all cases, where there is a deviation, the theory appears to overestimate the density of ions in the vicinity of the shell. For large q, an improved agreement can be achieved by increasing the screening parameter which reduces multi-particle interactions; e.g., for tetravalent ions the analytical prediction works very well for $\kappa = 1$ nm^{-1}, corresponding to 100 mM of 1:1 salt (black circles).

A similar trend is observed when the sign of surface charge density of the shell, σ, turns negative. In this case, a large increase is obtained (by up to a few orders of magnitude relative to the bulk concentration, c_0) in the surface density of tetravalent ions when the surface charge density is only modestly increased from $\sigma = -0.05$ e_0/nm^2 to $\sigma = -0.4$ e_0/nm^2 (Fig. 1d). The theory again works at sufficiently low $|\sigma|$ and breaks down at larger values. Note that the deviation between the theory and simulations can be tuned further by changing the screening parameter: the validity of the theory for $\sigma = -0.4$ e_0/nm^2 is restored (not shown) [16] if the screening parameter is increased to $\kappa = 1.73$ nm^{-1}, equivalent to 300 mM of 1:1 salt. The break-down of the theory is more dramatically observed at $\kappa = 0.58$ nm^{-1} with both limits falling well within the experimentally relevant values. Thus, the applicability of the above analytical predictions depends on all three parameters, q, σ and κ [16].

While the density of the multivalent ions *across* the shell surface can be understood within the phenomenology of the dressed multivalent-ion theory, the behavior in the lateral directions *along* the shell surface can be less so. The pair distribution function (pdf) of multivalent ions along the surface (Fig. 2a) indeed shows a noticeable *correlation hole* when plotted in terms of the lateral distance between multivalent ions, which results from the repulsion between ions residing at the vicinity of the shell. The size of the correlation hole, $a_\perp$, is consistent with the naive estimate $a_\perp \sim \sqrt{q e_0/|\sigma|}$ (being around 2.2 nm for the parameters in Fig. 2a), which can follow from a local electroneutrality argument for surface ions [7]. More remarkably, however, in the regime where the accumulation of the ions at the shell surface is highly enhanced and the theory breaks down (Fig. 1), we find a short-range ordering of multivalent ions along the surface clearly exhibited by a pronounced correlation peak in the pdf of multivalent ions. This behavior illustrates the fact that the failure of the dressed multivalent-ion theory is driven by the formation of a strongly correlated surface layer of multivalent ions, which incorporates many-body effects and is thus absent from the presented theory.

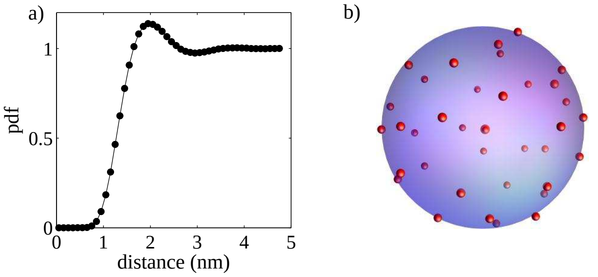

FIG. 2: (Color online) a) Normalized pair distribution function of multivalent ions from MC simulations for $R = 2.5$ nm, $\sigma = -0.8\,e_0/\mathrm{nm}^2$, $\kappa = 1\,\mathrm{nm}^{-1}$, $q = 4$. b) A typical simulated snapshot showing multivalent ions in the vicinity (within 1Å) of the shell for $R = 2.5$ nm, $\sigma = -1.6\,e_0/\mathrm{nm}^2$, $\kappa = 1.73$ nm^{-1}, $q = 4$. For these parameters, the shell experiences a total negative pressure of (a) $-0.28\ k_\mathrm{B}T/\mathrm{nm}^3$ and (b) $-1.31\ k_\mathrm{B}T/\mathrm{nm}^3$.

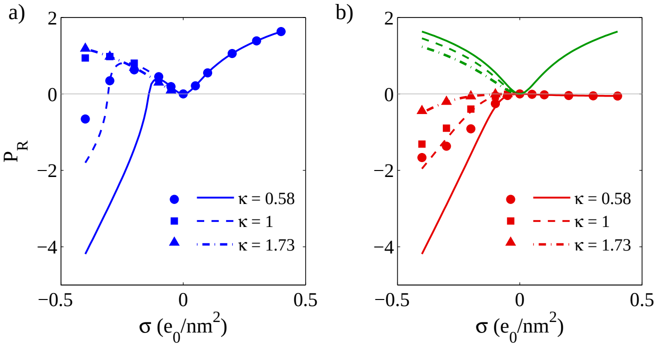

FIG. 3: (Color online) a) Rescaled total electrostatic pressure $P_R = \mathrm{sgn}(P') \times \log_{10}(1 + 100\,|P'|)$ (where $P' = P/P_0$ with $P_0 = 1\ k_\mathrm{B}T/\mathrm{nm}^3$) from simulations (symbols) and the dressed multivalent-ion theory (lines) as a function of σ for $R = 2.5$ nm, $q = 4$, $c_0 = 1$ mM, and different values of κ. b) Same as (a) but here we show different components of the total pressure due to shell's self-energy, P_{DH} (green, upper lines) and multivalent ions, P_q (red symbols and red, lower lines).

The electrostatic pressure acting on the shell also shows interesting variation depending on the system parameters. In Fig. 3a we plot the rescaled pressure, P_R, as a function of the surface charge density of the shell for tetravalent ions and $R = 2.5$ nm (the rescaling is done in such a way that the negative and positive values of pressure can be shown in a log-linear scale and points of zero pressure are correctly represented). For positively charged capsids, the pressure is always positive. In this case there is excellent agreement between analytical prediction (blue lines) and simulations. For negatively charged capsids, both the theory and simulations turn out to give *negative* pressure for screening parameters in the vicinity of the physiological value or smaller, indicating that the shell is being *compressed.* In this case the theory again tends to overestimate the mag-

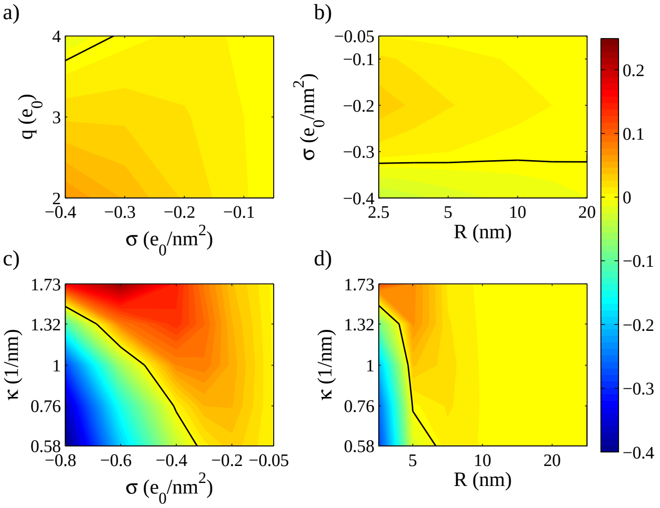

FIG. 4: (Color online) "Phase diagrams" showing regions of positive and negative electrostatic pressure acting on the shell in terms of the system parameters, q and σ (shown in linear scale) as well as R and κ (shown in logarithmic scale). Solid lines show the line of zero pressure. In a) we have fixed $R = 2.5$ nm and $\kappa = 0.58\,\mathrm{nm}^{-1}$, in b) we have fixed $q = 4$ and $\kappa = 0.58\,\mathrm{nm}^{-1}$, in c) $q = 4$ and $R = 2.5$ nm, and in d) we have fixed $q = 4$ and the total shell charge $Q_\sigma = 4\pi\sigma R^2 = -126\ e_0$ (e.g., we have $\sigma \simeq -0.1\ e_0/\mathrm{nm}^2$ for $R = 10$ nm).

nitude of the negative pressure and shows deviations from the simulations (compare symbols and lines in Fig. 3a). When the contribution due to the self-energy of the shell P_{DH} is subtracted, one obtains the pressure imparted on the shell by multivalent ions, P_q, which is shown by red symbols (simulations) and lines (theory) in Fig. 3b. Clearly, the negative pressure thus results purely from multivalent ions and then only when the shell is overall negatively charged. This negative pressure is directly related to the attractive interactions mediated by highly charged ions between equally charged surfaces [14]; it in fact results from summing up attractive forces along the outer and inner surfaces of the charged shell that have a component of the force directed towards the inside of the shell [16]. The sign of osmotic pressure acting on the shell is thus straightforwardly related to correlation attractions as seen in other strongly charged systems [7].

Note that an important factor determining the sign of the pressure is the bulk concentrations of multivalent as well as monovalent ions, as codified by κ, which can lead to a change of sign of the total pressure due to an increase in the negative pressure from the multivalent ions. In Fig. 4 we thus plot "phase diagrams" of the pressure acting on the shell as obtained from our MC simulations in terms of the parameters q, σ, κ, and R. We show regions where the pressure is negative and/or positive, with the black solid line indicating the *separatrix* of zero pressure. It is thus clear that by changing the system parameters one can reach a point where the electrostatic self-repulsion of the capsid is overcome and gives way to an inward force isotropically compressing the capsid.

The sign and magnitude of the pressure are both crucial in assessing the capsid stability towards shrinking and/or swelling. Sufficiently large negative pressure can lead to inward buckling of the capsid through a sequence of shrinking elastic instabilities [17], expected to occur when negative pressure is large enough, exceeding a critical value of $P_c \sim -5$ [atm] $\times$ (30 [nm]$/R)^3$ in magnitude. Our results indicate that in the range of $\sigma \sim -0.5$ e_0/nm^2 and $c_0 \sim 1$ mM, this type of destabilization and inward buckling may take place for large shells with radius $R > 150$ nm, an estimate that could however be lowered significantly by increasing the concentration of multivalent ions [16]. On the other hand, the change of sign of the pressure on complete removal of multivalent ions that turns the negative pressure to positive, would lead to swelling of the capsid and possibly outward buckling, destabilizing it towards swelling [6]. Multivalent ions can thus be implicated in both types of instabilities, leading to larger effects for larger sized capsids. Interestingly in this context, larger viruses such as mimivirus, megavirus, etc., with sufficiently large radii all seem to have either an external or an internal lipid membrane [18] that could serve as a local reservoir for multivalent ions acting in either direction. In general, local multivalent salt concentration gradients generated by a semipermeable membrane, could also play an important role in regulating the stability of other enveloped viruses.

Negative osmotic pressure also leads to important consequences for self-assembly of viral shells. Clearly for $P > 0$, the size of the capsid spontaneously increases, precluding a stable state with a finite R. On the other hand for $P < 0$, there could be two conceivable outcomes. In this regime strong electrostatic coupling will provide effective attractive interactions between equally charged capsomers, thus promoting their aggregation but not necessarily also their self-assembly into a fully formed capsid. A disordered aggregate might be a more stable configuration then an ordered spherical shell, indicating that salt and multivalent ion concentration could affect the strength of effective lateral interaction between capsomers and thus interfere with self-assembly. There are indications, mostly for divalent salts, that this is indeed what happens and that solution conditions (n_0 of salt, q, and c_0 of multivalent ions) do play an important role in the assembly/disassembly process [2, 6].

A.N. acknowledges support from the Royal Society, the Royal Academy of Engineering, and the British Academy. A.L.B. and R.P. acknowledge support from the ARRS Grants No. P1-0055 and J1-4297.

---

[*] Email: `a.naji@ipm.ir`

[1] A. Šiber, A. Lošdorfer Božič and R. Podgornik, Phys. Chem. Chem. Phys. **14**, 3746 (2012).

[2] R. Zhao, A. T. Hadfiled, M. J. Kremer and M.G. Rossman, Virology **227**, 13 (1997).

[3] P. Carrivain, A. Cournac, C. Lavelle, A. Lesne, J. Mozziconacci, F. Paillusson, L. Signon, J.-M. Victor and M. Barbi, Soft Matter **8**, 9285 (2012).

[4] H. S. Savithri, S. K. Munshi, S. Suryanarayana, S. Divakar and M. R. N. Murthy, J. Gen. Virol. **68**, 1533 (1987).

[5] A. S. Tyms, in *The Physiology of Polyamines*, Vol. II, edited by U. Bachrach and Y. M. Heimer (CRC Press, 1989).

[6] M.G. Rossman and J.W. Eriksson, in *Virus Structure and Assembly*, Ed. S. Casjens (1985), p.29.

[7] H. Boroudjerdi, Y. W. Kim, A. Naji, R. R. Netz, X. Schlagberger and A. Serr, Phys. Rep. **416**, 129 (2005).

[8] M. Kanduč, A. Naji, J. Forsman and R. Podgornik, J. Chem. Phys. **132**, 124701 (2010).

[9] T. S. Baker, N. H. Olson and S. D. Fuller, Microbiol. Mol. Biol. Rev. **63**, 862 (1999).

[10] A. Lošdorfer Božič, A. Šiber and R. Podgornik, J. Biol. Phys. **38**, 657 (2012).

[11] N. Steinmetz and M. Manchester, *Viral Nanoparticles: Tools for Materials Science and Biomedicine* (Pan Stanford Publishing, 2011).

[12] I. Yildiz, I. Tsvetkova, A. M. Wen, S. Shukla, H. Masarapu, B. Dragnea and N. Steinmetz, RSC Advances **2**, 3670 (2012).

[13] M. de Frutos, S. Brasiles, P. Tavares and E. Raspaud, Eur. Phys. J. E **17**, 429 (2005).

[14] M. Kanduč, A. Naji, J. Forsman and R. Podgornik, Phys. Rev. E **84**, 011502 (2011).

[15] A. Šiber and R. Podgornik, Phys. Rev. E **76**, 061906 (2007).

[16] L. Javidpour, A. Lošdorfer Božič, A. Naji and R. Podgornik, unpublished.

[17] A. Šiber and R. Podgornik, Phys. Rev. E **79**, 011919 (2009).

[18] P. Colson, X. de Lamballerie, G. Fournous and D. Raoult, Intervirology **55**, 321 (2012).